Stochastic model of partial discharge activity in liquid and solid dielectrics

A. L. Kupershtokh[1], C. Stamatelatos[2] and D. P. Agoris[2]

[1] Lavrentyev Institute of Hydrodynamics of Siberian Branch of Russian Academy of Sciences
Novosibirsk, 630090, Russia
[2] University of Patras, GR 26500 Rion, Greece

Abstract: **A new model that can simulate the main stochastic features of partial discharge activity at AC and DC voltages was proposed. In our simulations the narrow peaks of current were observed at the moment of every microdischarge in voids in solid dielectric after AC voltage was applied. The behavior of single cavity in dielectric liquid under DC voltage was also simulated.**

INTRODUCTION

Small gas-filled cavities existing in solid and liquid dielectrics can influence on electric strength and on life time of equipment. The inception of microdischarges in cavities is controlled by the local electric field rather than the average applied field. The gas inside the cavities has much lower electric strength than liquid or solid dielectrics. Moreover, electric field strength inside cavities is higher than that outside. Often, the equivalent circuit modeling approach (based on lumped capacitances) is used to study the behavior of embedded cavities in solid dielectrics [1,2].

Partial discharge (PD) activity has principally stochastic character. Stochastic features of partial discharges appear in variations of moments of PD events and of magnitude of peaks of current. Hence, the corresponding methods must be used for simulating of this process.

Since some period after microdischarge, the discharge extinguished due to surface charges appeared at the surface of the void.

In present work we proposed a new model that can simulate the main stochastic features of partial discharge activity at AC voltage.

ELECTROHYDRODYNAMICS

Hydrodynamic equations are the continuity equation

$$\frac{\partial \rho}{\partial t} + \nabla(\rho \mathbf{u}) = 0, \qquad (1)$$

and the Navier-Stokes equation

$$\frac{\partial \rho \mathbf{u}}{\partial t} + \nabla \Pi^{(0)}_{\alpha\beta} = \mathbf{F} + \eta \nabla^2 \mathbf{u} + (\zeta + \frac{\eta}{3}) \mathrm{grad}\, \mathrm{div}\, \mathbf{u}. \qquad (2)$$

Here, ρ is the density of liquid, $\mathbf{u}$ is the velocity of fluid flow, $\Pi^{(0)}_{\alpha\beta} = p\delta_{\alpha\beta} + \rho u_\alpha u_\beta$ is the non-viscous part of the momentum flux tensor.

Equations for concentrations n_i of carriers of electric charge are

$$\frac{\partial n_i}{\partial t} + \nabla(n_i \mathbf{u}) = D_i \Delta n_i - \mathrm{div}(\frac{q_i}{|q_i|} b_i n_i \mathbf{E}) + w_i - r_i . \qquad (3)$$

Here, D_i are the diffusivities, b_i are the macroscopic effective mobilities of charges carriers q_i; w_i, r_i are the rates of ionization and recombination of charge carriers (were neglected in bulk of dielectric in this work).

The Poisson's equation for potential of electric field φ is

$$\mathrm{div}(\varepsilon \nabla \varphi) = -4\pi q, \qquad \mathbf{E} = -\nabla \varphi , \qquad (4)$$

Here ε is the permittivity, $q = \sum q_i n_i$ is the electric charge density.

The electric force acting on the space charge in a liquid is

$$\mathbf{F} = q\mathbf{E} = -q \nabla \varphi . \qquad (5)$$

The electric current could be expressed as

$$\mathbf{j} = \sum (q_i n_i \mathbf{u} - D_i q_i \nabla n_i + b_i |q_i| n_i \mathbf{E}) = q\mathbf{u} - \sum D_i q_i \nabla n_i + \sigma \mathbf{E} , \qquad (6)$$

Here, the local conductivity $\sigma = \sum b_i |q_i| n_i$ depends on local concentrations of charge carriers and can be not constant in space and in time.

In the case of constant and equal coefficients $D_i = D$, multiplying (3) by q_i and summing over all i, we obtain

$$\frac{\partial q}{\partial t} + \nabla(q\mathbf{u}) = D\Delta q - \mathrm{div}(\sigma \mathbf{E}) . \qquad (7)$$

In our calculations the value of conductivity σ was taken to be constant.

METHOD OF SPLITTING

To solve the system of equations (1), (2), (4), (5) and (7) the method of splitting on physical processes [3] is used. The whole time step is divided into several stages implemented sequentially. These stages are

1. Modeling of hydrodynamic flows.
2. Simulation of convective transport and diffusion of charge carriers ($\partial q / \partial t + \nabla(q\mathbf{u}) = D\Delta q$).
3. Calculation of electric potential and charge transfer due to mobility of charge carriers.

0-7803-8954-9/05/$20.00©2005 IEEE.

4. Calculation of electrostatic forces acting on space charges in liquid.
5. Simulation of phase transition or interaction between immiscible liquids.
6. Simulation of partial discharges inside cavities.

The lattice Boltzmann equation (LBE) method was used for modeling the hydrodynamic flows and also for simulation of convective transport and diffusion of charge carriers [4,5]. The exact difference method (EDM) [5] was used to take into account the body force term in LBE method.

SIMULATION OF PHASE TRANSITION

Phase transitions were simulated in LBE method using the method of Zhang and Chen [6]. To simulate phase transition layer, the special force acting on the matter in every node was introduced. This force should be a gradient of certain potential U to ensure the global momentum conservation law (if external forces are absent)

$$\mathbf{F}_{\mathrm{N}} = -\nabla U \,. \tag{8}$$

Zhang and Chen proposed to express this potential using the equation of state as

$$U = P(\rho, T) - \rho\theta \,. \tag{9}$$

Here $\theta = kT/m = 1/3$ is the reduced temperature that is appropriate to isothermal LBE method used.

We proposed new approximation for method of Zhang and Chen. If we define some function

$$\varphi = \sqrt{-U} \,, \tag{10}$$

then we obtain the equation for force acting on the matter in the node

$$\mathbf{F}_{\mathrm{N}} = 2\varphi(\rho)\nabla\varphi(\rho) \,. \tag{11}$$

This form of force is similar to that used in the method of Shan and Chen [7,8]. For example, the following finite-difference approximation of the resulting force was used in [7,8] for one-dimensional case

$$F_i = G_0 \psi(\rho_i) \frac{\left(\psi(\rho_{i+1}) - \psi(\rho_{i-1})\right)}{h} \,. \tag{12}$$

In [7,8], the equation of state for one-dimensional case assumed to be $P = \rho\theta - G_0\psi^2(\rho)$. For this equation of state, the approximation (8) can be written in the form

$$F_i = G_0 \frac{\left[\psi(\rho_{i+1}) + \psi(\rho_{i-1})\right]}{2} \frac{\left[\psi(\rho_{i+1}) - \psi(\rho_{i-1})\right]}{h} \,. \tag{13}$$

The only difference is between (12) and (13). The local value of function $\psi(\rho_i)$ in considered node i is used in (13) instead of mean value of the left and the right values in (12).

We proposed new more general finite-difference approximation of (8) and (11) in the form of linear combination of (12) and (13) with some coefficient A

$$F_i = \left[A\varphi(\rho_{i+1}) + (1-2A)\varphi(\rho_i) + A\varphi(\rho_{i-1})\right] \frac{\left(\varphi(\rho_{i+1}) - \varphi(\rho_{i-1})\right)}{h} \,. \tag{14}$$

This formula is valid for arbitrary form of equation of state if use (9) and (10).

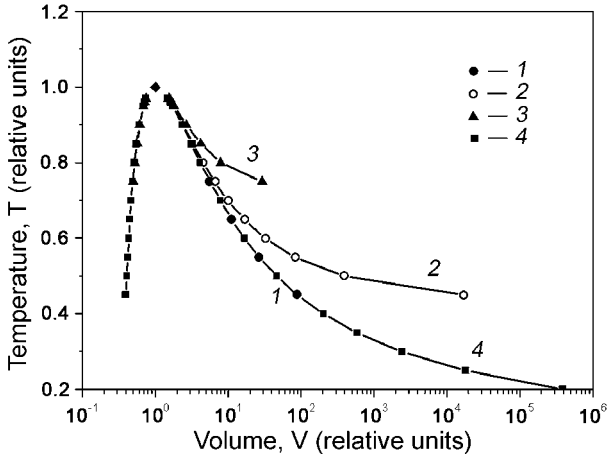

Fig.1. The coexistence curve for van der Waals equation of state.

The coexistence curve for van der Waals type equation

$$P = k\left(\frac{8T\rho}{3-\rho} - 3\rho^2\right) \tag{15}$$

at $k = 0.01$ (coefficient of system of units) is shown in Fig. 1. Curve *1* – theoretical calculations in accordance with the Maxwell rule for the equation of state, curve *2* – the approximation similar to (12), curve *3* – the approximation similar to (13). The deviations of the approximation (14) (curve *4*) from the theoretical values (curve *1*) is less then 0.2% at $A = -0.152$ in the range from critical point down to $T = 0.4$. The exact difference method (EDM) [5] was used for all approximations to take into account the body force term.

For two-dimensional D2Q9 LBE model, we proposed the following approximation

$$F^x_{i,j} = \frac{2}{3h}\Big\{(A\varphi_{i+1,j} + (1-2A)\varphi_{i,j} + A\varphi_{i-1,j})(\varphi_{i+1,j} - \varphi_{i-1,j}) + \\ + \frac{1}{4}\Big[(A\varphi_{i+1,j+1} + (1-2A)\varphi_{i,j} + A\varphi_{i-1,j-1})(\varphi_{i+1,j+1} - \varphi_{i-1,j-1}) + \\ + (A\varphi_{i+1,j-1} + (1-2A)\varphi_{i,j} + A\varphi_{i-1,j+1})(\varphi_{i+1,j-1} - \varphi_{i-1,j+1})\Big]\Big\}. \tag{16}$$

The similar expression was used for y component of force.

MODEL OF PARTIAL DISCHARGES

In the present work we used three models of pulse conductivity. The simplest criterion of microdischarge inception is the well-known field threshold criterion (FTC) $E > E_*$, where E is the local electric field strength. This criterion is essentially deterministic. To describe the

stochastic nature of partial discharge inception inside cavities, two stochastic criteria were used. The first is the field fluctuation criterion (FFC) [9,10,11]. If the condition $E > E_* - \delta$ was fulfilled in a cavity, then the gas inside the cavity became conductive with conductivity σ_0. An exponential probability distribution for fluctuation δ was used $\varphi(\delta) = \exp(-\delta / g)/g$ which is equivalent to $\delta = -g\ln(\xi)$. Hereafter, ξ will be a random number uniformly distributed in the interval from 0 to 1. The second is the MESTL (multi-element stochastic time lag) criterion [10,11]. For all cavities i that were in nonconductive state, the stochastic time lags of microdischarge inception $\Delta t_i = -\ln(\xi_i)/r(E)$ were calculated. The growth probability function $r(E)$ depends on local electric field inside the cavity. During one time step Δt, the microdischarges occur in all cavities for which $\Delta t_i < \Delta t$. The gas inside these cavities became conductive with constant conductivity σ_0.

If the electric field inside cavity decreased down to the value that is less than some critical value $E_{\rm cr}$, we assumed that the microdischarge terminated and conductivity became equal to zero (complete decay of plasma inside cavity due to reducing the energy release in comparison with energy loss).

To obtain the distributions of electric-field potential φ and, correspondingly, of electric field $\mathbf{E}$ in the region between electrodes, the system of electrodynamics equations (4) for quasi-stationary case was solved at each time step together with the equations of conductive transport of charge

$$\frac{\partial q}{\partial t} = -\mathrm{div}\,\mathbf{j}, \qquad \mathbf{j} = \sigma \cdot \mathbf{E}. \qquad (17)$$

We supposed that the conductivity σ and the current density $\mathbf{j}$ exist only inside the cavities ($\sigma = 0$ in dielectrics outside cavities).

Transport of electric charge due to conductivity was calculated in parallel with solving of Poisson equation. The time-implicit finite-difference equations for charge transport equation and for Poisson equation were solved by the method of iterations relatively values q^{n+1} and φ^{n+1} at the next time step at every node, as it was done in [10]

$$q^{n+1} = q^n + \tau\,\mathrm{div}\left(\sigma\nabla\varphi^{n+1}\right), \quad \mathrm{div}(\varepsilon\nabla\varphi^{n+1}) = -4\pi q^{n+1}. \quad (18)$$

SIMULATION RESULTS

Partial discharges in solid dielectrics

The system of set of cavities randomly distributed in bulk of solid dielectric between point-plane electrodes was studied. The dielectric was stressed by AC voltage higher that the inception voltage of partial discharges. The MESTL criterion and function $r(E) = BE^3$ were used. We registered in our simulations the current in external circuit. The narrow peaks were observed at the moment of every microdischarge. Typical plot obtained in computer simulations is shown in Fig. 2.

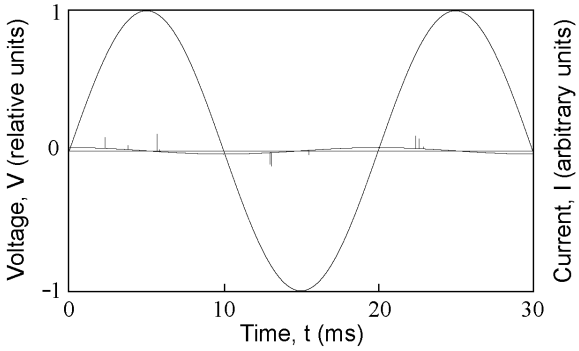

Fig.2. Partial discharge activity during three half periods of voltage.

The behavior of coupled cavities was also simulated. The influence of microdischarge in cavity on probability of inception of microdischarges in very neighbor cavities was demonstrated.

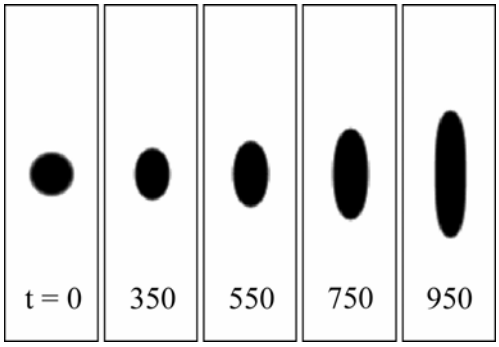

Fig.3. The behavior of single spherical vapor cavity in dielectric liquid stressed by constant DC test-voltage. Dark color corresponds to lower density. Frame size 55×200 lattice units.

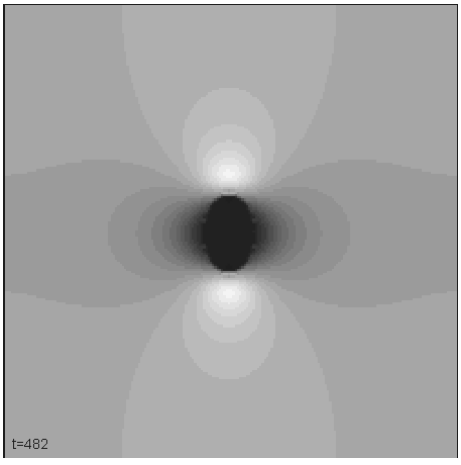

Fig.4. Distribution of vertical component of electric field inside and outside vapor bubble at the moment after microdischarge. Dark color corresponds to lower values of electric field. Lattice size 200×200.

Partial discharges in vapor cavity embedded in dielectric liquid

The behavior of single spherical cavity in dielectric liquid stressed by constant DC test-voltage was also simulated. The electric strength of gases is much lower than that of liquids. Hence, the electric breakdown can occur if the vapor bubble is greater that a certain critical size. After breakdown, the bubble becomes conductive, and it is deformed under the action of electric forces. The dynamics of bubble deformation and growth is shown in Fig. 3. We used FTC criterion for microdischarge inception ($E_* = 2E_{\rm cr}$) in this simulation.

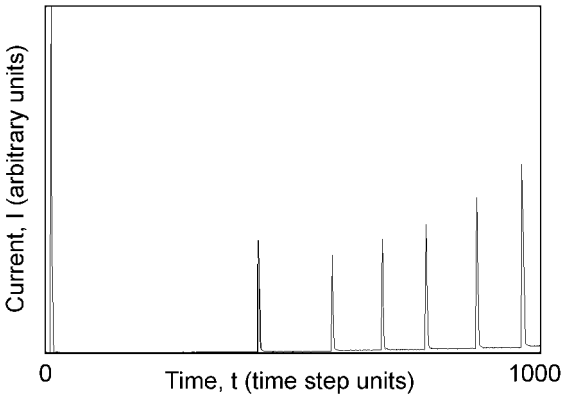

Fig.5. Partial discharges in single vapor bubble embedded in dielectric liquid stressed by constant DC test-voltage. FTC criterion for microdischarges.

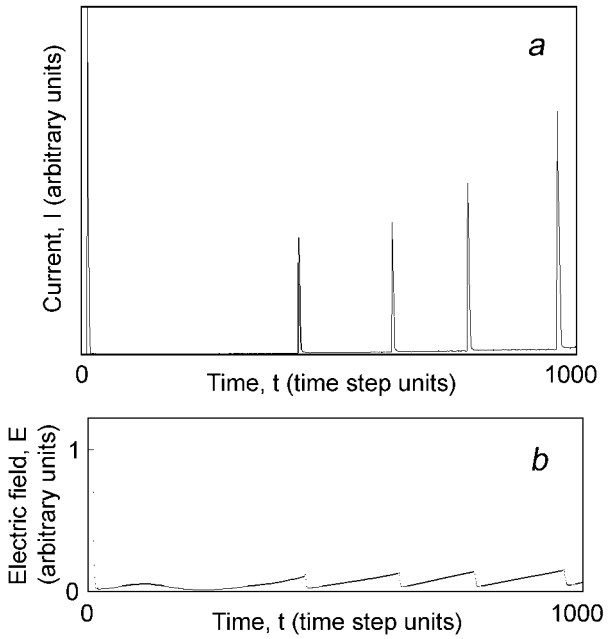

Fig.6. (*a*) Partial discharges in single vapor bubble embedded in dielectric liquid stressed by constant DC test-voltage. FFC criterion for microdischarges ($E_* = 4E_{\rm cr}$, $g = 0.1E_*$). (*b*) Electric field strength in the central part of the bubble.

The distribution of vertical component of electric field inside and outside vapor bubble at the moment after microdischarge is shown in Fig. 4. The currents in external circuit are shown in Fig. 5 (FTC) and 6*a* (FFC). The first microdischarge occurred since a very short delay after voltage applied. As expected, the magnitudes of the next peaks are much lower than of the first. The slowly increase component of the current was present due to growth of the bubble (Fig. 3) that carried charges at the surface. The electric field strength in the central part of the bubble is shown in Fig. 6*b*.

ACKNOWLEDGMENT

This work was supported by the Russian Foundation for Basic Research (grant No. 05-02-17092).

REFERENCES

[1] A. Gemant and W. Von Philipoff, “Die Funkenstrecke mit Vorkondensator,” *Zeitschrift für Technische Physik*, vol. 13, pp. 425-430, 1932.

[2] D. P. Agoris and N. D. Hatziargyriou, “Approach to partial discharge development in closely coupled cavities embedded in solid dielectrics by lumped capacitance model,” *IEE Proceedings – A*, vol. 140, no. 2, pp. 131-134, March 1993.

[3] N. N. Yanenko, *The method of fractional steps.* Berlin: Springer, 1967.

[4] A. L. Kupershtokh and D. A. Medvedev, “Lattice Boltzmann equation method in electrohydrodynamic problems,” in *Proc. 5th Int. Workshop on Electrohydrodynamics*, Poitiers, France, 2004, pp. 61–65.

[5] A. L. Kupershtokh, “New method of incorporating a body force term into the lattice Boltzmann equation,” in *Proc. 5th Int. Workshop on Electrohydrodynamics*, Poitiers, France, 2004, pp. 241–246.

[6] R. Zhang and H. Chen, “Lattice Boltzmann method for simulations of liquid-vapor thermal flows,” *Phys. Rev. E.*, vol. 67, no. 6, p. 066711, 2003.

[7] X. Shan and H. Chen, “Lattice Boltzmann model for simulating flows with multiple phases and components,” *Phys. Rev. E.*, vol. 47, no. 3, pp. 1815–1819, 1993.

[8] X. Shan and H. Chen, “Simulation of nonideal gases and liquid-gas phase transitions by the lattice Boltzmann equation,” *Phys. Rev. E.*, vol. 49, no. 4, pp. 2941–2948, 1994.

[9] A. L. Kupershtokh, “Fluctuation model of the breakdown of liquid dielectrics”, *Sov. Tech. Phys. Lett.* vol. 18, no. 10, pp. 647–649, 1992.

[10] D. I. Karpov and A. L. Kupershtokh, “Models of streamer growth with "physical" time and fractal characteristics of streamer structures,” in *Conf. Record of the 1998 IEEE Int. Symp. on Electrical Insulation, IEEE No. 98CH36239,* Arlington, USA, 1998, pp. 607-610.

[11] A. L. Kupershtokh, V. Charalambakos, D. Agoris and D. I. Karpov, “Simulation of breakdown in air using cellular automata with streamer to leader transition,” *J. Phys. D: Appl. Phys.*, vol. 34, no. 6, pp. 936–946, 2001.